Japanese Journal of Applied Physics
Vol. 47, No. 4, 2008, pp. 3220–3225

Retinal Stimulation on Rabbit Using Complementary Metal Oxide Semiconductor Based Multichip Flexible Stimulator toward Retinal Prosthesis

Takashi TOKUDA, Ryosuke ASANO, Sachie SUGITANI, Mari TANIYAMA, Yasuo TERASAWA[1], Masahiro NUNOSHITA, Kazuaki NAKAUCHI[2], Takashi FUJIKADO[2], Yasuo TANO[2], and Jun OHTA

Graduate School of Materials Science, Nara Institute of Science and Technology, 8916-5 Takayama, Ikoma, Nara 630-0192, Japan
[1]*Vision Institute, NIDEK Co., Ltd., 73-1 Hama, Gamagori, Aichi 443-0036, Japan*
[2]*Department of Ophthalmology, Osaka University Medical School, 2-15 Yamadaoka, Suita, Osaka 565-0871, Japan*

(Received October 2, 2007; accepted December 10, 2007; published online April 25, 2008)

The Functionality of a complementary metal oxide semiconductor (CMOS) LSI-based, multichip flexible retinal stimulator was demonstrated in retinal stimulation experiments on rabbits. A 1 × 4-configured multichip stimulator was fabricated for application to experiments on animals. An experimental procedure including surgical operations was developed, and retinal stimulation was performed with the fabricated multichip stimulator. Neural responses on the visual cortex were successfully evoked by the fabricated stimulator. The stimulator is confirmed to be applicable to acute animal experiments.
[DOI: 10.1143/JJAP.47.3220]

KEYWORDS: retinal prosthesis, CMOS stimulator, multichip architecture

1. Introduction

LSI-based neural interfacing/rehabilitation/prosthesis technology is one of the research fields in which electronics technology can provide new and powerful solutions.[1–4] Retinal prosthesis technology is a biomedical application for which LSI-based devices can play an essential role.[5–16] For cases of retinitis pigmentosa (RP) and age-related macular degeneration (AMD), it is reported that only photoreceptor cells are impaired and other neural layers partially remain. Retinal prosthesis is a neural prosthesis technology that aims to provide a substitutional visual sensation with patterned electric stimulation of the visual nerve system. A number of projects developing retinal prosthesis systems using different technical approaches are now under way in Japan, the United States, Germany, and other countries.[5–16]

Compared with an electrode array fabricated on a flexible substrate with printed patterns, the LSI-based stimulator is a powerful platform for high-resolution retinal stimulation. To realize a flexible LSI-based retinal stimulator, we proposed to configure a flexible retinal stimulator with an array of small LSI stimulators (unit chip) that can be operated cooperatively. We have reported on the design, packaging, and functional characterization of a multichip retinal stimulator.[13–16]

In this work, we designed a new unit chip and assembled it into a flexible stimulator for retinal stimulation of a rabbit's eye. We developed an experimental procedure including surgical implant operations, and performed retinal stimulation of an anesthetized rabbit's eye. Many works have been reported on *in vivo* retinal stimulation for application to retinal prosthesis.[10–12] However, *in vivo* retinal stimulation using an LSI-based stimulator has been hardly reported. We describe in detail the retinal stimulation of a rabbit's retina, and present the results obtained showing the functionality of the fabricated multichip flexible retinal stimulator.

2. Fabrication of Multichip Flexible Stimulator for Animal Experiments

Figure 1 shows the concept of a multichip flexible retinal stimulator. A small multielectrode complementary metal oxide semiconductor (CMOS) stimulator, "unit chip", is mounted on a flexible substrate with appropriate spacing. With this structure, the stimulator can be bent between unit chips. Currently, each unit chip is a single-site stimulator with addressable stimulation electrodes.

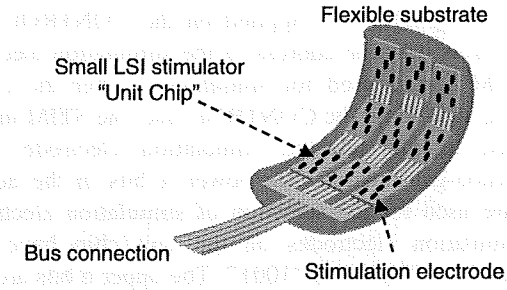

Fig. 1. Concept of multichip flexible retinal stimulator.

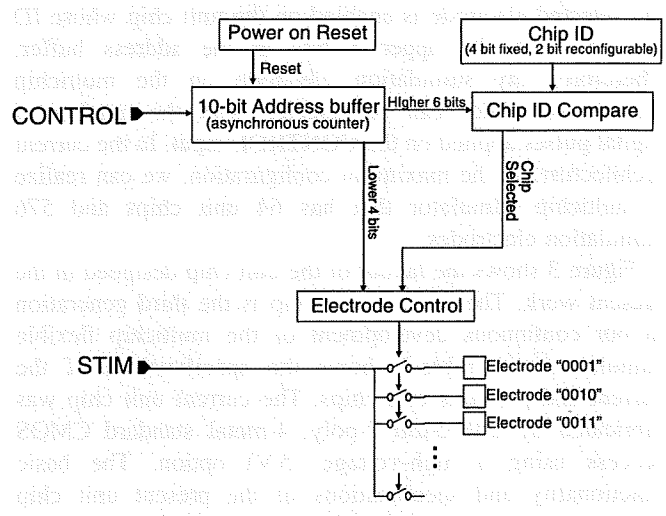

Fig. 2. Block diagram of unit chip.

Figure 2 shows a block diagram of the unit chip. The unit chip has nine stimulation output pads and four control inputs: VDD, GND, CONTROL, and STIM. The VDD and GND lines are used for continuous power supply, and the operation voltage of the unit chip is DC 5 V. The CONTROL

Table I. Specifications of unit chips designed in present and previous studies.

	Present (Third generation)	Previous[15,16] (Second generation)	Previous[13,14] (First generation)
Fabrication process	0.35 μm 2-poly 4-metal standard CMOS	0.35 μm 2-poly 4-metal standard CMOS	0.6 μm 2-poly 3-metal standard CMOS
Unit chip size (μm^2)	600 × 600	600 × 600	600 × 600
Series resistance (Ω)	~200	~200	~1 × 10^3
Reset sequence	Power on reset	Power on reset	Logic
Number of electrodes per unit chip	9	9	9
Address space for unit chip (bit)	6	6	4
(Maximum number of unit chips)	(64)	(64)	(16)
Maximum number of electrodes in multichip stimulator	576	576	144
Number of reconfigurable bits in chip ID (bit)	2/6	6/6	0/4

line is used for addressing. The unit chip has a 10-bit asynchronous counter for the address buffer. It counts the number of digital pulses applied on the CONTROL input and interprets it as the address of the stimulation electrode. The STIM line is used for stimulation. After the control pulses are applied on the CONTROL line, the STIM input is connected to the selected stimulation electrode via a transmission-gate switch. The lower 4 bits in the address buffer are used for the selection of stimulation electrodes. The stimulation electrodes on the unit chip have 4-bit addresses from "0000" to "1001". The upper 6 bits are used to choose one of the unit chips assembled on the flexible stimulator. Each unit chip has a 6-bit unique ID for identification. The connection between the STIM input and the selected electrode is enabled on the unit chip whose ID matches with the upper 6 bits in the address buffer. Therefore, any stimulation electrode on the multichip flexible stimulator can be selected with the number of digital pulses applied on the CONTROL input. In the current architecture, in the maximum configuration, we can realize a multichip stimulator that has 64 unit chips and 576 stimulation electrodes.

Figure 3 shows the layout of the unit chip designed in the present work. The current unit chip is the third generation in our continuous development of the multichip flexible stimulator.[13–16] Table I shows the specifications of the current and previous unit chips. The current unit chip was fabricated by a 0.35 μm 2-poly, 4-metal standard CMOS process using a high-voltage (5 V) option. The basic functionality and specifications of the present unit chip (third generation) are the same as those of the chip in the second generation, and their detailed description was presented in our previous reports.[15,16] As the only revised feature, the number of reconfigurable bits in the chip ID is reduced from 6 to 2. Thus, only the upper 2 bits of the 6-bit chip ID can be modified by fuse amputation. This is reasonable because we designed an LSI die on which 16 unit chips with chip IDs from "000000" to "001111" are aligned, and we can cover all chip IDs reconfiguring the highest 2 bits in the chip ID. The series resistance shown in Table I is an ON resistance of the CMOS switch (transmission gate) that establishes a connection between the STIM input and the selected electrode. The CMOS switch consists of a

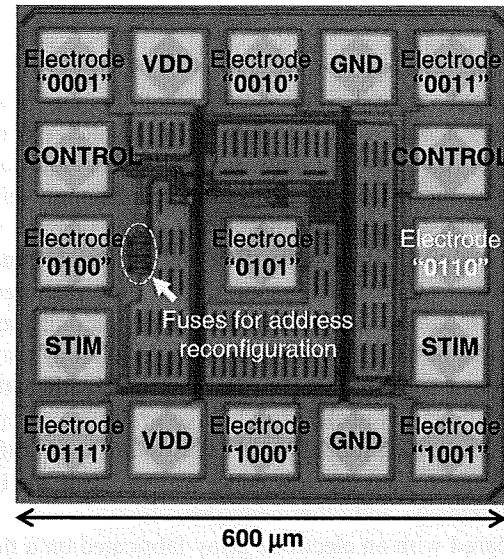

Fig. 3. Layout of unit chip.

parallel set of NMOS and PMOS transistors. In the first generation, the series resistance is as large as 1 kΩ, but it is reduced to a value less than 200 Ω in the unit chip in the second generation.[16] In the present design (the third generation), the CMOS switch circuitry is basically identical with that in the second generation.

Packaging is another essential issue using in the case of the CMOS-based device for bioimplant applications. The CMOS device must be molded in a waterproof and biocompatible material. In the present work, we aimed to realize a multichip stimulator durable for acute (less than several hours) animal experiments. We assembled a multichip flexible stimulator with the structure developed in the previous work.[16] Figure 4 shows the structure of the presentmultichip stimulator. The detailed packaging process for the device structure shown in Fig. 4 is described in ref. 16.

In this work, we chose a configuration with a 1 × 4 unit chip array, which matched the size of a rabbit's eye. Figure 5 show photographs of the multichip stimulator fabricated for functional demonstration in animal experiments using rabbits. As shown in Fig. 5, the device can be bent with a radius of curvature $r = 1.7$ mm, and the device can be fit on

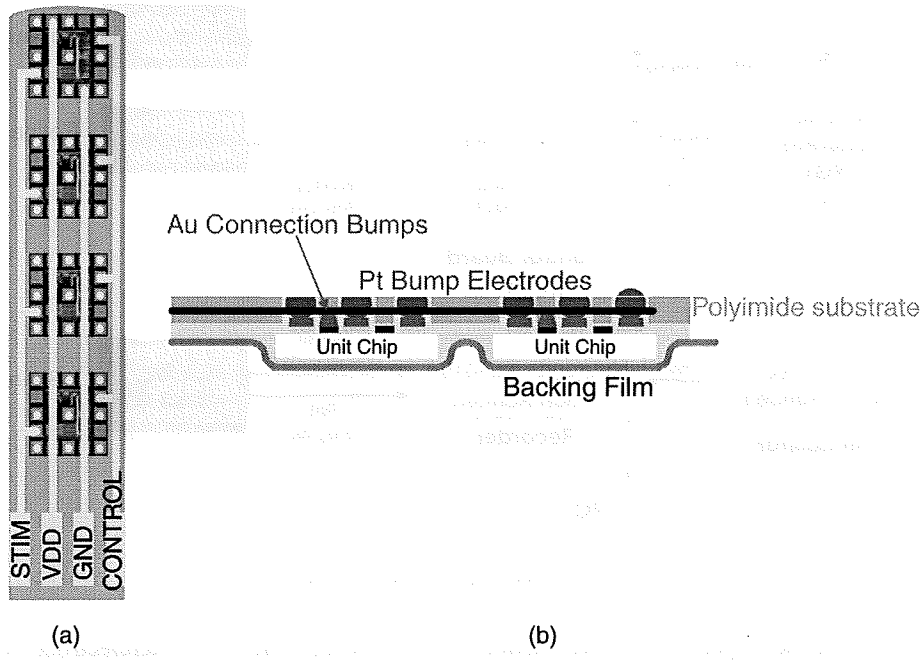

Fig. 4. Structure of multichip retinal stimulator: (a) plan view and (b) cross section.

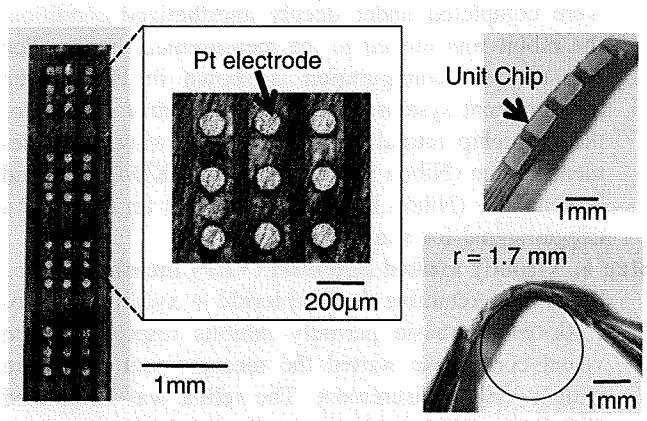

Fig. 5. Multichip flexible retinal stimulator for retinal stimulation experiments on rabbits.

a rabbit's eye. The diameter of the bulk Pt stimulation electrode is typically 90 μm, and the pitches of the stimulation electrodes are 240 (within the unit-chip) and 620 (between two adjacent unit chips) μm.

3. Stimulation Experiments on Rabbit's Retina Using the Multichip Flexible Stimulator

3.1 Experimental procedure

To demonstrate and characterize the functionality of the multichip flexible stimulator, we performed retinal stimulation experiments using rabbits. We confirmed that the fabricated multichip flexible stimulator can be surgically implanted in a rabbit's eye, and used for the stimulation of the retina. Response in the visual cortex of the brain was also recorded. Figure 6 schematically shows the configuration of the experiments on rabbits. Electrically evoked potential (EEP) measurement was performed by stimulating the retina with the present multichip stimulator [Fig. 6(a)]. Figure 6(b) shows the configuration of screw electrodes in the visual

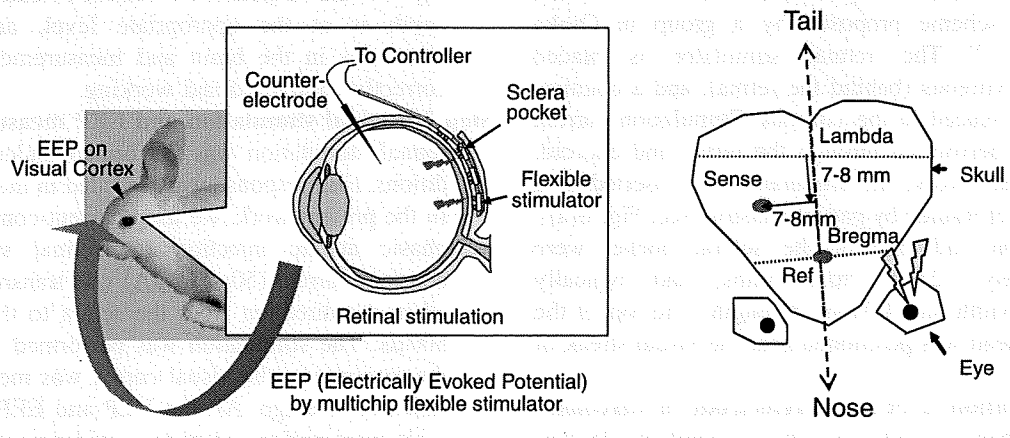

Fig. 6. (a) Experimental configuration and (b) positions of screw electrodes on skull for measurement.

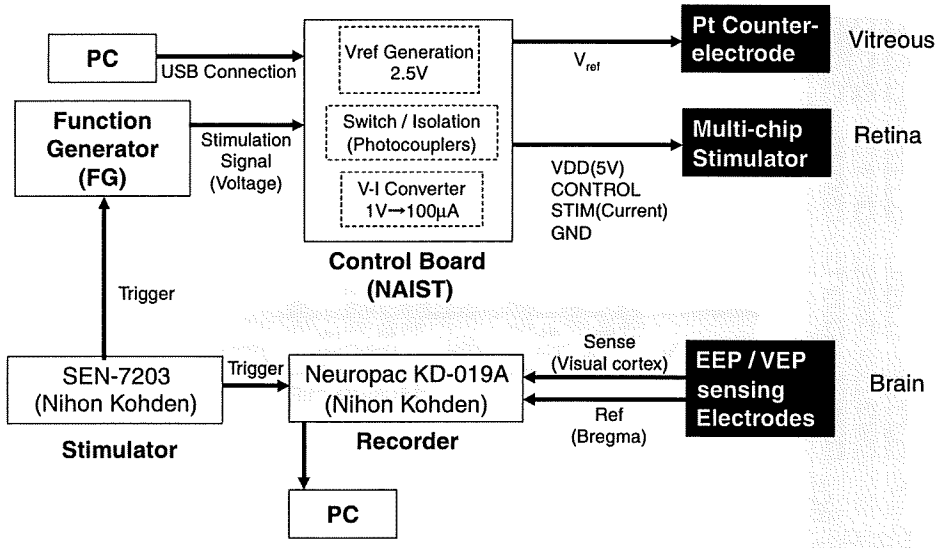

Fig. 7. Measurement setup for EEP/VEP measurement.

cortex for measurement. All the experiments were carried out following the Institutional Guidelines of Osaka University and the ARVO Resolution on the Use of Animals in Ophthalmic Research.

A non-SPF (specific-pathogen-free) Dutch belted rabbit with normal sight was used for the animal experiments. The experiments were carried out in a non-SPF part of an animal experimental facility. The experimental procedure was as follows.

Step 1. Anesthesia: The rabbit was anesthetized with an intramuscular injection of ketamine hydrochloride (50 mg/kg) and xylazine hydrochloride (5 mg/kg), which provides stable anesthesia for more than 2 h. Additional injections were also carried out to control appropriate anesthesia depth.

Step 2. Implantation of screw electrodes for measurement: Stainless-steel screw electrodes were implanted into the visual cortex through the skull to measure the response to retinal stimulation. The position of the sensing electrode is shown in Fig. 6(b). And the reference electrode was implanted into the bregma.

Step 3. Implantation of multichip flexible stimulator: A 1×4-configured multichip retinal stimulator was implanted and fixed in a suprachoroidal transretinal stimulation (STS) configuration. STS is a retinal stimulation scheme proposed by a group in Osaka University.[17,18] The retinal stimulator is placed outside the vitreous (behind the retina), and a counter-electrode is placed in the vitreous. Stimulation current injection is performed through the retina and choroid. In the present work, the stimulator was inserted in a scleral pocket formed by partial incision [see, Fig. 6(a)]. The position and size of the scleral pocket were approximately 12 mm from limbs, and typically 2.0 mm in width and 4.0 mm in length. The top of the stimulator head was positioned near the visual streak of the eye.

Step 4. Implantation of Pt counterelectrode in vitreous: A polyurethane-coated wire Pt counterelectrode was inserted into the vitreous. The coating layer at the end of the wire was removed, and the Pt counterelectrode was exposed. The Pt counterelectrode was inserted into the sclera. The distance between the insertion point and the limbus was approximately 1 mm.

Step 5. Connection of the stimulator and electrodes to measurement system: After all the surgical operations were completed under deeply anesthetized condition, the rabbit was moved to the measurement bench. The measurement configuration is shown in Fig. 7. The measurement system consisted of a control system for the multichip retinal stimulator, brain wave measurement system (Nihon Kohden Neuropac KD-019A), and a stimulator (Nihon Kohden SEN-7203) for generate a trigger signal for stimulation.

Step 6. Visually evoked potential (VEP) measurement: Since the ketamine hydrochloride + xylazine hydrochloride anesthesia partially inhibits response in the visual cortex, we started the measurement procedure with a VEP measurement. The retina was stimulated with flushing light and response in the visual cortex was measured. A flush bulb (1.2 J) was placed approximately 15 cm from the cornea. The stimuli were provided at 0.5 Hz, and triggered recording was performed. The response was measured 20–30 times and averaged to suppress random noise in the measurement. By checking the VEP response, we confirmed that the anesthesia depth is at the appropriate level, and the screw electrodes in the brain and measurement system are correctly configured and working.

Step 7. Retinal stimulation and EEP measurement: The retinal stimulation was performed under various conditions. EEP response was recorded in the visual cortex. In the present work, we used current-controlled, monophasic anodic injection for retinal stimulation. A constant current (50–500 μA) was transretinally injected in the direction from the sclera to the vitreous for 500 μs. The stimulation was performed at 0.5 Hz, and the response in the visual cortex was measured 20–30 times on average. All the VEP and EEP experimental trials were performed under environmental room light. Environmental room light may cause a small VEP in the visual cortex. However, we have detected no environ-

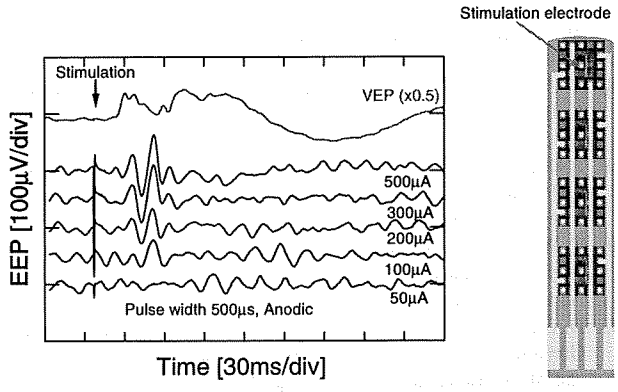

Fig. 8. EEP responses obtained in single-site stimulation trial.

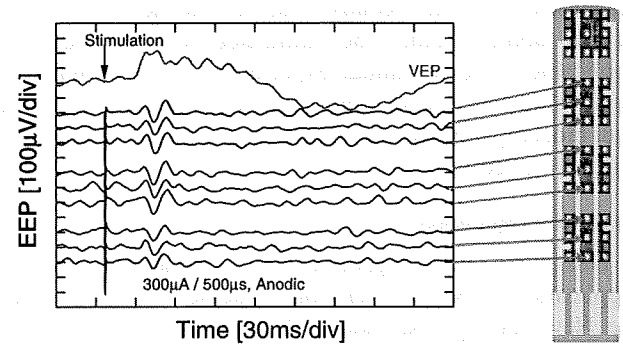

Fig. 9. EEP responses obtained in multichip, multisite stimulation trial.

mental-room-light-induced VEP in the measured VEP and EEP traces, since the brightness of the environmental room light is extremely smaller than that used in VEP measurement.

3.2 *Results*

We performed two kinds of stimulation experiments to demonstrate the functionality of the multichip flexible stimulator. One is a single-site stimulation trial performed with different stimulation strengths, and the other is a multisite, multichip stimulation trial with a constant stimulation strength.

3.2.1 *Single-site stimulation with different stimulation strengths*

To confirm that response in the visual cortex can be evoked under reasonable conditions, we performed single-site stimulation with different stimulation strengths. We fixed the pulse duration at 500 μs, and varied current in the range of 50–500 μA. Figure 8 shows the EEP traces observed in the single-site stimulation. Clear EEP responses were obtained for stimulation currents in the range 100–500 μA. The total charge, charge density, and current density for the threshold condition (100 μA, 500 μs) are 50 nC/pulse, 620 μC/cm^2, and 1.23 A/cm^2. The current/duration and charge for the stimulation are considered to be within typical ranges for the current-controlled retinal stimulation. We can conclude that the present multichip retinal stimulator can be successfully used for experimental applications to retinal prosthesis.

There is a typical difference between the observed VEP and EEP responses. In the VEP traces, peaks tend to fuse. We consider the following reasons for this difference. In the VEP trials, stimulation light excites visual cells in the retina, and neural excitation is transferred to the retinal network layer via synaptic connections. The signal transfer path for VEP includes the response of the visual cells to the stimulation light, and with more synaptic connections the peaks in VEP traces tend to fuse. This mechanism is also supported by the difference in latency, the temporal interval between the stimulation and first the response observed in the brain wave traces. Some EEP traces (for instance, 500 μA stimulation in Fig. 8) have a small peak with a latency of approx. 15 ms, which is smaller than the latency in the VEP traces (19 ms, in Fig. 8).

In the present work, no severe damage was observed in either the rabbit's eyes or the Pt electrodes, owing to the small number of stimulation trials performed in one procedure. However, it should be noted that the waveform (monophasic and charge-unbalanced) and charge density in the present work are inappropriate for chronic retinal stimulation from the viewpoint of safety for both biological tissues and electrode materials.

3.2.2 *Multichip and multisite stimulation with constant strength*

Figure 9 shows the EEP responses obtained in the multichip, multisite stimulation trial. We sequentially performed stimulations using different stimulation electrodes on the center column of the 1 × 4 multichip retinal stimulator (see inset of Fig. 9). Note that the top unit chip was not used in this trial, owing to the error in the packaging process. The pulse conditions were 300 μA/500 μs. As shown in Fig. 9, clear EEP responses were observed in the multichip stimulation trial. Since the stimulator head is not pressed onto the inside of the scleral pocket, a thin electrolyte layer is expected to exist between the stimulation electrodes and the scleral tissue. Furthermore, in the present work, the positions of the multichip stimulator and screw electrodes in the visual cortex are not coordinated each other. This means that a clear positional dependence of the EEP responses should not be expected yet. However, EEP traces in Fig. 9 show a weak dependence on stimulation position. The amplitude observed in the EEP responses corresponding to the electrodes on the unit chip at a large insertion depth was larger than that observed for the other unit chips. This result is quite promising and we can expect application of the multichip stimulator in a two-dimensional stimulation trial. The localization of the visual sensation, which will be one of the essential issue in retinal prosthesis technology, is expected to be demonstrated by EEP measurement with a higher spatial resolution in the visual cortex.

4. Conclusions

A CMOS LSI-based, multichip flexible retinal stimulator was used in stimulation experiments on a rabbit's retina. A 1 × 4-configured multichip stimulator was fabricated for animal experiments. An experimental procedure including surgical operations was developed. Retinal stimulation was performed with the fabricated multichip stimulator, and EEP

responses were successfully observed in the visual cortex of the rabbit's brain. The stimulator is confirmed to be applicable to acute animal experiments. In the future, the development of flexible stimulators with improved durability and biocompatibility for longer experimental applications will be carried out.

Acknowledgements

This work was supported by a Grant for Practical Application of Next-Generation Strategic Technology from the New Energy and Industrial Technology Development Organization (NEDO), Japan, and by Health and Labor Sciences Research Grants from the Ministry of Health, Labour, and Welfare of Japan.

1) K. Najafi and K. D. Wise: IEEE J. Solid-State Circuits **21** (1986) 1035.
2) J. Ji, K. Najafi, and K. D. Wise: IEEE Trans. Biomed. Eng. **38** (1991) 75.
3) T. Kawano, Y. Kato, R. Tani, H. Takao, K. Sawada, and M. Ishida: IEEE Trans. Electron Devices **51** (2004) 415.
4) E. Margalit, J. D. Weiland, R. E. Clatterbuck, G. Y. Fujii, M. Maia, M. Tameesh, G. Torres, S. A. D'Anna, S. Desai, D. V. Piyathaisere, A. Olivi, E. de Juan, and M. S. Humayun: J. Neurosci. Methods **123** (2003) 129.
5) W. Liu, K. Vichienchom, M. Clements, S. C. DeMarco, C. Hughes, E. McGucken, M. S. Humayun, E. de Juan, J. D. Weiland, and R. Greenberg: IEEE J. Solid-State Circuits **35** (2000) 1487.
6) S. C. DeMarco, W. Liu, P. R. Singh, G. Lazzi, M. S. Humayun, and J. D. Weiland: IEEE J. Solid-State Circuits **38** (2003) 1679.
7) D. Palanker, A. Vankov, P. Huie, and S. Baccus: J. Neural Eng. **2** (2005) S105.
8) E. Zrenner, A. Stett, S. Weiss, R. B. Aramant, E. Guenther, K. Kohler, K. D. Miliczek, M. J. Seiler, and H. Haemmerle: Vision Res. **39** (1999) 2555.
9) J. Deguchi, T. Watanabe, T. Nakamura, Y. Nakagawa, T. Fukushima, S. J.-Chill, H. Kurino, T. Abe, M. Tamai, and M. Koyanagi: Jpn. J. Appl. Phys. **43** (2004) 1685.
10) T. Watanabe, R. Kobayashi, K. Komiya, T. Fukushima, H. Tomita, E. Sugano, H. Kurino, T. Tanaka, M. Tamai, and M. Koyanagi: Jpn. J. Appl. Phys. **46** (2007) 2785.
11) D. Güven, J. D. Weiland, G. Fujii, B. V. Mech, M. Mahadevappa, R. Greenberg, R. Roizenblatt, G. Qiu, L. LaBree, X. Wang, D. Hinton, and M. S. Humayun: J. Neural Eng. **2** (2005) S65.
12) J. F. Rizzo III, J. Wyatt, J. Loewenstein, S. Kelly, and D. Shire: Invest. Ophthalmol. Vis. Sci. **44** (2003) 5355.
13) J. Ohta, N. Yoshida, K. Kagawa, and M. Nunoshita: Jpn. J. Appl. Phys. **41** (2002) 2322.
14) T. Tokuda, Y.-L. Pan, A. Uehara, K. Kagawa, M. Nunoshita, and J. Ohta: Sens. Actuators A **122** (2005) 88.
15) J. Ohta, T. Tokuda, K. Kagawa, T. Furumiya, A. Uehara, Y. Terasawa, M. Ozawa, T. Fujikado, and Y. Tano: IEEE Eng. Med. Biol. Mag. **25** (2006) 47.
16) T. Tokuda, S. Sugitani, M. Taniyama, A. Uehara, Y. Terasawa, K. Kagawa, M. Nunoshita, Y. Tano, and J. Ohta: Jpn. J. Appl. Phys. **46** (2007) 2792.
17) H. Kanda, T. Morimoto, T. Fujikado, Y. Tano, Y. Fukuda, and H. Sawai: Invest. Ophthal. Visual Sci. **45** (2004) 560.
18) K. Nakauchi, T. Fujikado, H. Kanda, T. Morimoto, J. S. Choi, Y. Ikuno, H. Sakaguchi, M. Kamei, M. Ohji, T. Yagi, S. Nishimura, H. Sawai, Y. Fukuda, and Y. Tano: Graefes Arch. Clin. Exp. Ophthalmol. **243** (2005) 169.

CMOS-Based Multichip Networked Flexible Retinal Stimulator Designed for Image-Based Retinal Prosthesis

Takashi Tokuda, *Member, IEEE*, Kohei Hiyama, Shigeki Sawamura, Kiyotaka Sasagawa, *Member, IEEE*, Yasuo Terasawa, Kentaro Nishida, Yoshiyuki Kitaguchi, Takashi Fujikado, Yasuo Tano, and Jun Ohta, *Member, IEEE*

***Abstract*—We propose and characterize a CMOS LSI-based neural stimulator for retinal prosthesis technology. The stimulator is based upon a multichip architecture in which small-sized CMOS stimulators named "unit chips" are organized on a flexible substrate. We designed a unit chip with an on-chip stimulator and light-sensing circuitry. We verified that all the functions implemented on the unit chip worked correctly and that an organized unit chip can be used as a retinal stimulator with multisite image-based patterned stimulation. We also demonstrated light-controlled retinal stimulation for the first time in an *in vivo* animal experiment on a rabbit's retina.**

***Index Terms*—Biomedical, CMOS biomedical device, image sensor, neural stimulator, retinal prosthesis.**

I. Introduction

In the biomedical engineering field, interest in and expectations for CMOS LSI-based implantable electronics are growing larger and larger. Sensory prosthesis technology such as retinal prosthesis is a field in which bio-implantable electronics are expected to be essential solutions. Retinal prosthesis aims to provide a substitutional visual sensation by evoking with electric stimulation the signal pathway between the retina and the brain [1]–[20]. Currently, most research work pursuing retinal prosthesis approaches the problem by stimulating the remaining retinal cells on the degenerated retinal tissue (retinal stimulation). This approach is applicable to patients suffering from age-related macular degeneration or retinitis pigmentosa, in which mainly the photoreceptor cells are damaged and other cells remain.

In contrast to cochlear implants, which have been a big success in the bio-implantable electronics field, retinal prosthesis confronts a lot of technical difficulties. It is generally accepted that CMOS LSI-based stimulators will be in demand at the realization stage of retinal prosthesis technology. However, the retina is soft, and its tissue is spherically curved. The retinal stimulator for retinal prosthesis technology must be flexible and spherically bendable.

Only a few groups have reported functional demonstrations of CMOS LSI-based retinal stimulators. Furthermore, although there are many development projects aiming to realize light-controlled (image-based) retinal prosthesis in which the stimulation is triggered or controlled based upon the light intensity detected at the stimulation site, no demonstration on light-controlled stimulation *in vivo* has been reported to our knowledge.

We have been developing CMOS LSI-based flexible retinal stimulators based upon a multichip architecture [13]–[18]. We performed an acute implantation of the multichip flexible stimulator onto a rabbit's eye and successfully observed electrically evoked potential (EEP) in the visual cortex of the rabbit's brain [18]. The stimulators in our previous reports were designed for single-site stimulation using an external stimulator. No current generator was implemented on the CMOS stimulator, and we could not perform multisite stimulation. Light-controlled functionality was not implemented on the device either.

In the present work, we developed CMOS stimulator chips which are potentially compatible with the following: 1) multisite stimulation; 2) light-controlled stimulation; and 3) spherical packaging. We describe the functional and chip design in Section II. The functional verifications are presented in Section III. In Section IV, we describe a functional demonstration of the image-based patterned current injection emulated in a "dry" situation. In Section V, we perform an *in vivo* demonstration of light-controlled retinal stimulation in an animal experiment using a rabbit.

Manuscript received January 7, 2009; revised June 2, 2009. Current version published October 21, 2009. This work was supported in part by the Strategic Research Program for Brain Sciences in Japan, by the Research Grant Program of the Asahi Glass Foundation, Japan, by the Health and Labor Sciences Research Grant from the Ministry of Health, Labor, and Welfare of Japan, and by the VLSI Design and Education Center, The University of Tokyo, in collaboration with Cadence Design Systems, Inc. The review of this paper was arranged by Editor E. Fossum.

T. Tokuda, K. Sasagawa, and J. Ohta are with the Graduate School of Materials Science, Nara Institute of Science and Technology, Nara 630-0192, Japan (e-mail: tokuda@ms.naist.jp).

K. Hiyama was with the Graduate School of Materials Science, Nara Institute of Science and Technology, Nara 630-0192, Japan. He is now with the Corporate Manufacturing Engineering Center, Toshiba Corporation, 33, Yokohama 235-0017, Japan.

S. Sawamura was with the Graduate School of Materials Science, Nara Institute of Science and Technology, Nara 630-0192, Japan. He is now with Canon Inc., Tokyo 146-8501, Japan.

Y. Terasawa is with the Vision Institute, R&D Division, NIDEK Company, Ltd., Gamagori 443-0036, Japan.

K. Nishida, Y. Kitaguchi, and T. Fujikado are with the Graduate School of Medicine, Osaka University, Osaka 565-0871, Japan.

Y. Tano, deceased, was with the Graduate School of Medicine, Osaka University, Osaka 565-0871, Japan.

Color versions of one or more of the figures in this paper are available online at http://ieeexplore.ieee.org.

Digital Object Identifier 10.1109/TED.2009.2030552

II. Design of the Multisite Light-Controlled Stimulator Chip

It is generally accepted that a long-term retinal stimulation should be performed through charge-balanced injections into the target area of the retinal tissue. However, in practice, the optimum stimulation scheme and conditions have not yet been figured out. A current between 100 and 1000 μA with a pulse duration between 100 and 1000 μs is the typical range reported in the literature for the field [6]–[20].

In previous works, we developed a series of CMOS LSI-based retinal stimulators designed with a multichip architecture. With the multichip architecture, we assemble an array of small-sized CMOS stimulator chips (unit chips) on a flexible substrate with printed bus wiring. An appropriate spacing between the unit chips provides the flexibility of the stimulator [13]–[18].

The function of the previously developed multichip flexible stimulator was quite simple. The unit chip has nine addressable electrodes for stimulation, and the unit chip itself has its own ID. All the unit chips are connected in parallel on a four-wire bus line (including power supply lines), and one electrode on one unit chip can be selected using the addressing function. The stimulation signal was generated with an external stimulator (and isolator), and the retinal stimulator only relays the signal to the selected electrode.

In the present work, we designed a new multichip flexible stimulator that is compatible to a simultaneous multisite stimulation scheme. We totally redesigned the CMOS unit chip and implemented the following features.

1) To realize a simultaneous multichip stimulation, a bidirectional current generator was implemented as an on-chip stimulator.
2) The electrode configuration of the unit chip was changed from nine electrodes per unit chip to a single-electrode type.
3) Both the single-/multisite stimulation mode using an on-chip stimulator and the single-site relaying stimulation mode using an external stimulator are available.
4) Light-controlled stimulation was implemented.
5) The unit chips are connected on a five-channel bus wiring including VDD and GND lines.
6) The unit chips were designed in a preconnected and aligned configuration to provide spherical flexibility.

Fig. 1 shows the layout and block diagram of the unit chip developed in the present work. Table I shows its specifications. The size of the core is 200 μm $\times$ 200 μm. For functional extension, we added one digital input to increase the channel number of the bus to five. The five-channel bus consists of the following: VDD (5 V dc), GND (0 V), CONT1 (5 V digital), CONT2 (5 V digital), and STIM (analog). The main part of the unit chip consists of a control logic and a bidirectional stimulation current generator.

To realize the multichip stimulation functionality, the unit chip must be designed to discriminate between commands based upon the chip ID from the pulse train applied on CONT1 and CONT2.

Fig. 2 shows the operation sequence of the present unit chip. A simultaneous H (5 V) input for CONT1 and CONT2 is used to reset and restart all the unit chips. The CONT1 input is used mainly as a delimiter, and CONT2 is used to send values to the unit chips.

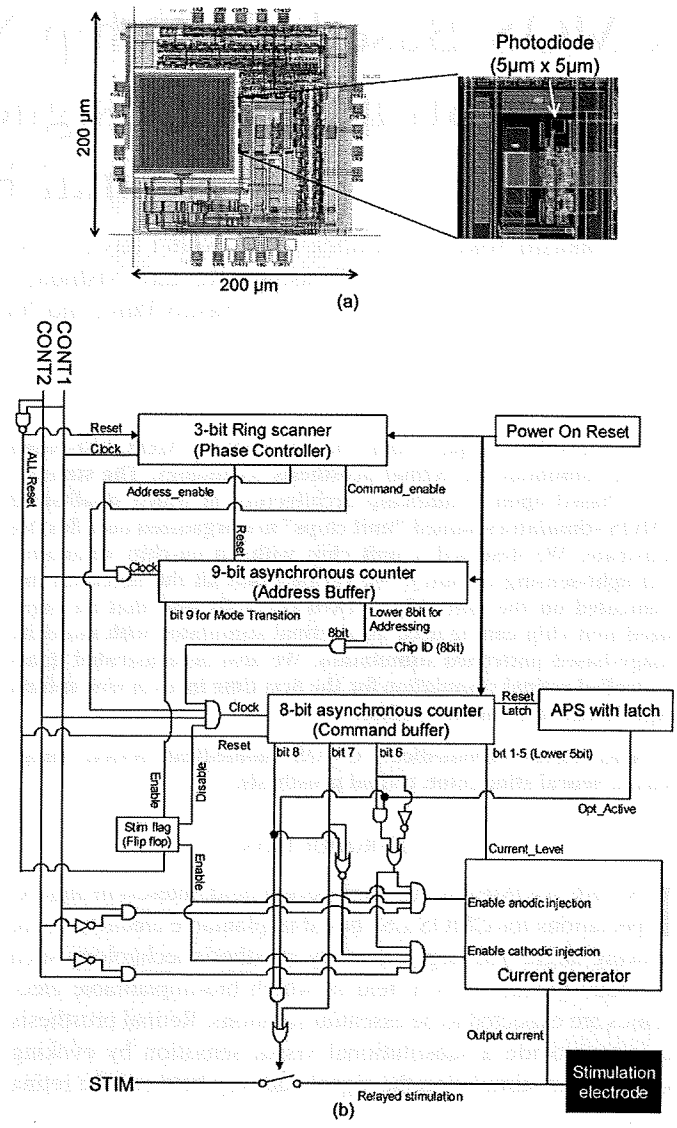

Fig. 1. Layout and block diagram of the unit chip for a multichip flexible retinal stimulator.

TABLE I
Specifications of the Unit Chip

Process	0.35 μm 2 poly 4 metal standard CMOS
Core size	200 μm × 200 μm
Number of stimulation Electrode	1
Size of stimulation electrode	100 μm × 100 μm
Photosensor	3 Tr. active pixel sensor
Photodiode size	5 μm × 5 μm
Input	VDD, GND, CONT1, CONT2, STIM
ID spece	8 bit (Max 256 unique IDs)
Operation voltage	5 V
Stimulation conditions	50–1050 μA, 50 μA step

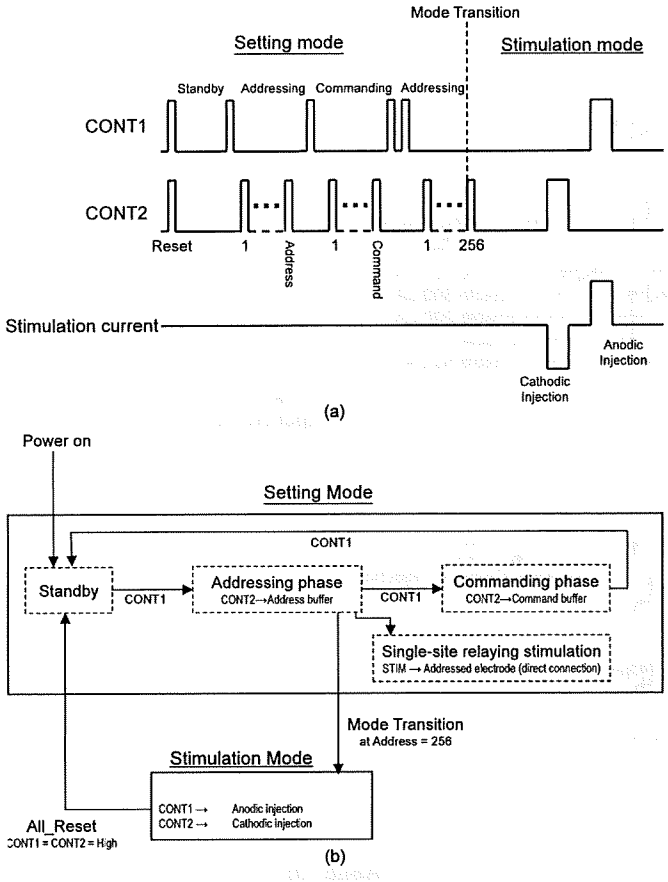

Fig. 2. Operation sequence for the unit chip.

As shown in Fig. 2, the unit chip has two operation modes. When the unit chip is reset, it is in the setting mode. Each unit chip accepts and stores a control command which defines the function to be used and the conditions for retinal stimulation. After we set the commands on the unit chips, we change the operation mode into a stimulation mode to perform retinal stimulation using the on-chip stimulator. The stimulation output is prohibited in the setting mode, except for single-site relaying stimulation which is described later.

In the setting mode, there are two listening phases: addressing and commanding. The listening phase is defined by a 3-b asynchronous ring scanner clocked by CONT1. At the beginning of the addressing phase, a 9-b asynchronous counter called the address buffer in the control logic is reset. All the unit chips then count the pulses applied to CONT2 and compare them to 8-b chip IDs that are unique to each unit chip. After the unit chip address is applied, the listening phase is changed into the commanding phase with a pulse on CONT1. In the commanding phase, the pulse applied on CONT2 is relayed to an 8-b counter called the command buffer only when the value in the address buffer is the same as the chip ID. The number of pulses for the CONT2 input is stored in the command buffer on the selected unit chip and interpreted as the specific operation condition provided for the unit chip. Table II shows the command table. The command includes the stimulation current for the on-chip stimulator and additional instructions. In contrast to the address buffer, the command buffer is not reset throughout the operation. After the pulses on CONT2, to define the operation conditions for the selected unit chip, we apply

TABLE II
COMMAND TABLE

Bit 1	Enable 50 μA
Bit 2	Enable 100 μA
Bit 3	Enable 200 μA
Bit 4	Enable 300 μA
Bit 5	Enable 400 μA
Bit 6	Enable light-controlled stimulation using on-chip stimulator
Bit 7	Enable light-controlled relaying stimulation using external stimulator
Bit 8	Enable unconditional relaying stimulation using external stimulator

*Default operation = unconditional stimulation using on-chip stimulator

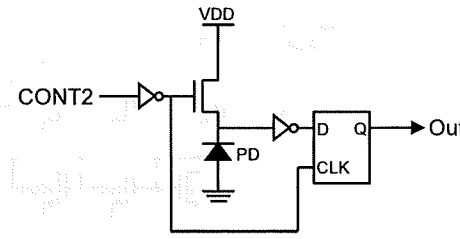

Fig. 3. Schematic for the light-controlled decision circuitry.

pulses on CONT1 to start another address and command for the next unit chip.

After we set the conditions for all the unit chips to be used for stimulation, we change the operation mode from the setting mode to the stimulation mode. To change the operation mode, the ninth bit of the address buffer is turned on H by applying 256 pulses on CONT2 in the addressing phase. Once the ninth bit becomes H, a 1-b flag resistor called a "stim flag" is put on H until the device is reset. Since the input of the command buffer is blocked in the stimulation mode, we can use CONT1 and CONT2 to trigger the stimulation. We use CONT1 and CONT2 to control the anodic and cathodic current injection. The stimulator was designed for symmetric injection, and the durations of the CONT1 and CONT2 pulses should be the same if we want to maintain charge balance during the stimulation.

Light-controlled stimulation is one of the most important functional extensions in the present design. We implemented a light-controlled decision for local stimulation, in which the stimulation is enabled when the local light intensity is higher than a threshold value. We implemented an active pixel sensor with binary output, shown in Fig. 3. The layout of the circuitry is shown in the inset in Fig. 1. The size of the photodiode was 5 μm × 5 μm. In contrast to conventional CMOS image sensor pixels, VDD was used as the reset voltage. Although this may cause nonlinearity in the sensitivity curve, we can implement the light-controlled functionality without any additional input. A comparator directly connected to the photodiode node transforms the photodiode level into a binary output. It is very important that the photodiode is reset and that the comparator is latched when CONT2 is low. The photodiode starts to discharge at the L-to-H transition for each pulse on CONT2, and the decision at the H-to-L transition of the pulse is latched until the next pulse is applied. This means that the

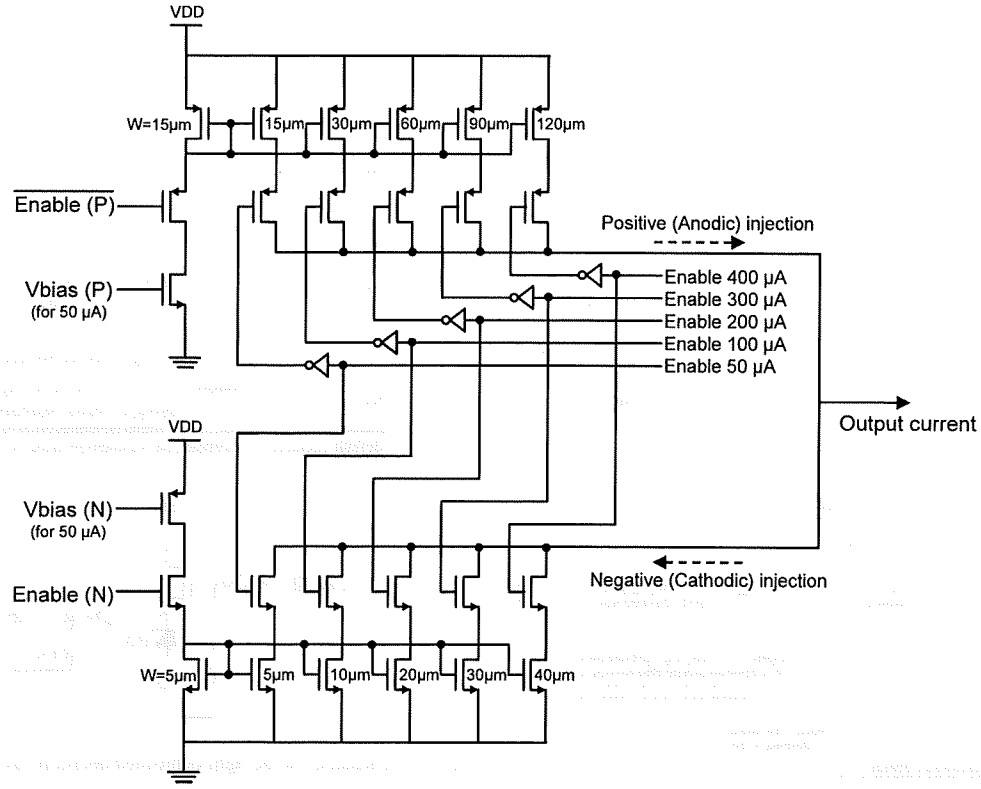

Fig. 4. Schematic for the bidirectional constant-current stimulator.

threshold light intensity for light-controlled decisions can be adjusted with the length of the last pulse in the commanding phase. We implemented both light-controlled and unconditional stimulation. When we perform the light-controlled decision for the stimulation, the length of the last pulse in the commanding phase is adjusted to provide the appropriate threshold.

The single-site relaying stimulation is implemented within the setting mode. Since the stimulation function is disabled in all the unit chips in the setting mode, we can realize single-site stimulation with no additional control to disable the other unit chips. The only control sequence for single-site relaying stimulation is to send the "direct connection" command to one of the unit chips. The "direct connection" function is activated when the seventh or eighth bit of the command buffer is set at H. The single-site relaying stimulation mode can be controlled by light as well.

We implemented a bidirectional current injector as the on-chip stimulator. Fig. 4 shows the schematic of the stimulator circuitry. The stimulator consists of a pair of NMOS and PMOS current sources. The gate widths of the MOS current regulators are designed to flow at 50, 100, 200, 300, and 400 μA. The injection current for the stimulation can be varied using combinations of these current regulators. The current regulator lines to be used are defined by the lower 5 b of the commend buffer (Enable 50 μA–Enable 400 μA). The injection switches of the selected current regulator lines in the PMOS current source are closed when CONT1 is H, and the injection switches in the NMOS current source are closed when CONT2 is H.

In the die design, we placed a set of unit chip cores with different chip IDs on one die. We used two kinds of connection structures. One is external pads around the unit chip core (pad type), and the other is preconnected wires which will be transformed into a flexible bus wiring (padless type). Using the external pads, the CMOS die is bonded onto a flexible

TABLE III
VARIATIONS OF THE RETINAL STIMULATOR CHIPS

Chip type	(a)	(b)	(c)
Layout	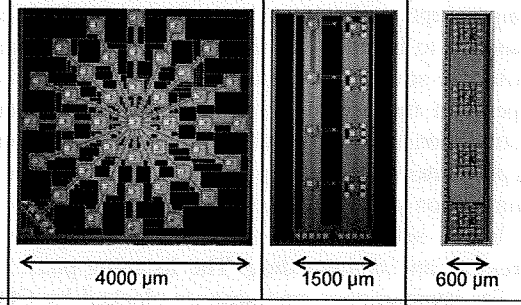 4000 μm	1500 μm	600 μm
Electrodes per unit chip	1		9
Stimulation	Multi-site		Single-site
On-chip stimulator	Implemented		Not implemented
Number of unit chips on die	41	4 x 2 types	4
Connection type	Padless	Pad / Padless	Pad
Light sensing cirucuit	This work (Fig. 3)		
Lifetime in wet environment	Not yet		Over 10 days
In vivo demonstration	Not yet		This work

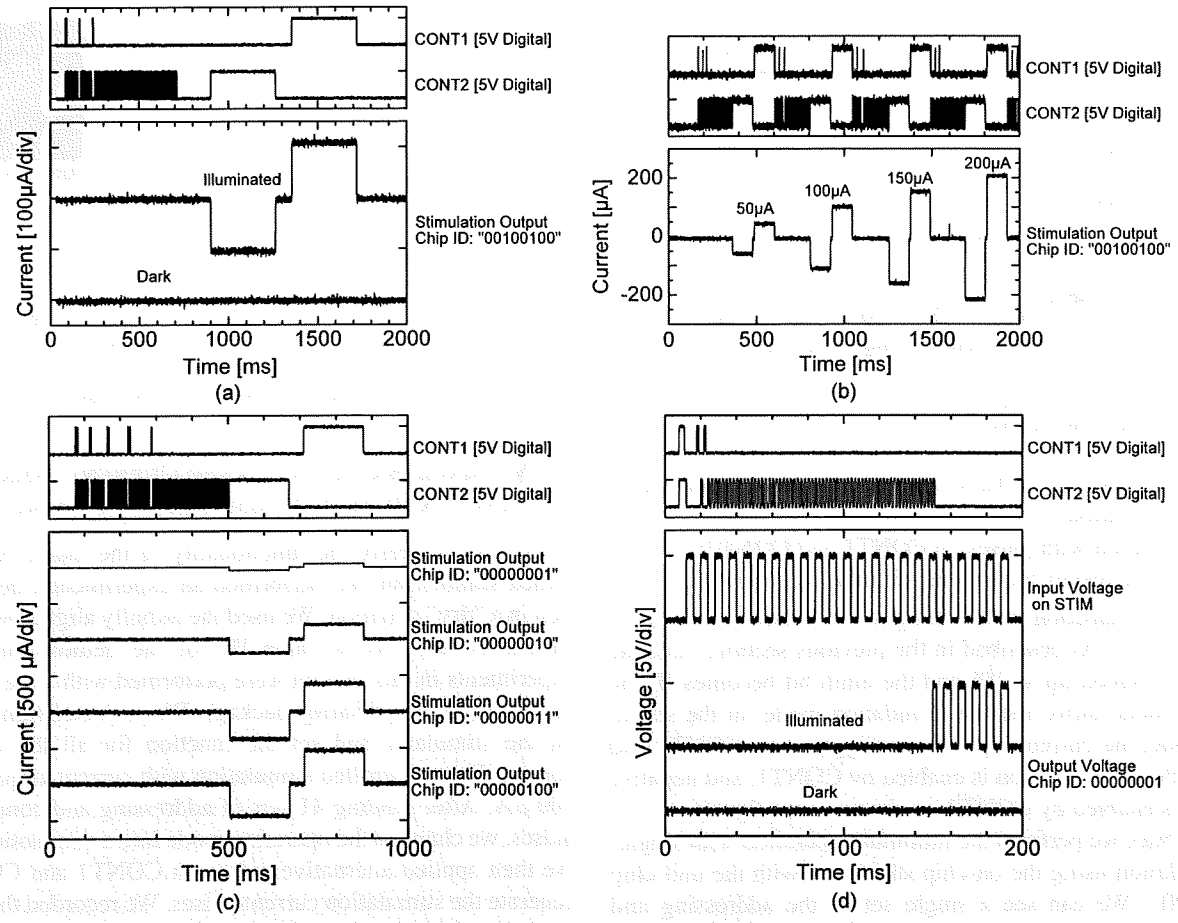

Fig. 5. Control and injection traces observed during the operation of the unit chips. (a) Biphasic current injection from a single unit chip using the on-chip stimulator. (b) Biphasic current injection from a single unit chip sequentially performed with different currents using the on-chip stimulator. (c) Biphasic current injection from four unit chips with different currents using the on-chip stimulator. (d) Connection measurement with a controlled voltage pulsed in the single-site relaying stimulation mode.

substrate with bus wirings and separated by a deep reactive ion etching process for flexible packaging [15]–[18]. We are also developing another connection structure using preconnected wires between the unit chips. We are developing this type of packaging to realize an improved form factor and better packaging yield. The detailed structure and packaging process shall be reported elsewhere.

In the present work, we designed three kinds of CMOS chips for functional verification and performance characterization. Table III shows the variations for the stimulator chips. The table includes the following: (a) a 41-unit radial stimulator; (b) a four-unit linear stimulator (two types of connection structures); and (c) a four-unit stimulator with the same design as previous works and the light-controlled stimulation developed in this paper.

III. Functional Characterization of the Unit Chip

Fig. 5(a)–(d) shows the experimentally obtained results showing the functions of the unit chip. Fig. 5(a)–(c) shows the operations using the on-chip stimulator. Fig. 5(a) and (b) was recorded using the unit chips with a chip ID of "00100100." In Fig. 5(c), we show the functionality of the multichip stimulation; the unit chips with IDs of "00000001," "00000010," "00000011," and "00000100" were used. Each stimulation electrode was connected to a voltage source kept at 2.5 V via a resistance of 2 kΩ. We have confirmed that the control logic of the present unit chip works at least up to a clock frequency of 40 MHz.

Fig. 5(d) shows the results of the single-site relaying stimulation mode using an external stimulator. Five-volt digital pulses are continuously applied on the STIM input of the unit chip, and the voltage of the stimulation electrode for the unit chip "00000001" was monitored.

The output traces are plotted in terms of current for operations using an on-chip stimulator [Fig. 5(a)–(c)] and in voltage for the single-site relaying stimulation mode [Fig. 5(d)].

In the demonstrations shown in Fig. 5(a)–(d), we can see the control sequences in the traces of CONT1 and CONT2. The control sequences consist of the value representing the number of pulses on CONT2 delimited by one or two pulses on CONT1. The sequences consist of the following:

1) reset with CONT1 = CONT2 = H;
2) input the address for the target unit chip (number of CONT2 pulses = target chip ID);
3) set the function and conditions for the stimulation (number of CONT2 pulses = command);
4) repeat steps 2) and 3) for all the unit chips to be used;

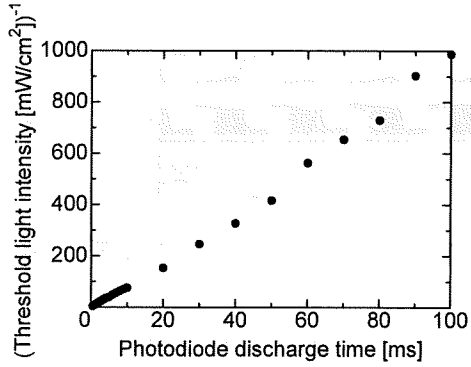

Fig. 6. Threshold light intensity as a function of the accumulation time for the light-controlled decision circuitry.

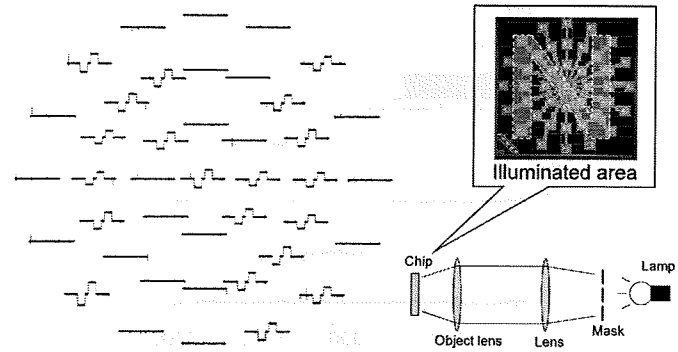

Fig. 7. Results of the image-based patterned current injection.

5) 256 pulses on CONT2 to transition the mode from control to stimulation;
6) stimulation with pulses on CONT1 and CONT2;
7) reset and restart for another stimulation procedure.

The mode transition from setting to stimulation is observed in Fig. 5(a)–(c). As described in the previous section, once the address is counted up to 256 and the ninth bit becomes H, the operation mode turns into the stimulation mode. In the stimulation mode, the current injection is triggered by CONT1 and CONT2. Positive injection is enabled by CONT1, and negative injection is enabled by CONT2, as shown in the figures.

In Fig. 5(a), we perform the minimum operation with single-site stimulation using the on-chip stimulator with the unit chip "00100100." We can see a single set of the addressing and commanding sequence on the CONT1 and CONT2 traces, followed by a single set of biphasic current injections controlled by CONT1 and CONT2.

In Fig. 5(b), we sequentially performed biphasic current injections with different conditions from the unit chip "00100100." The figure shows that the unit chip was correctly reset by the sequence CONT1 = CONT2 = H. We can change the condition even for each injection in the manner shown in Fig. 5(b).

In Fig. 5(c), we assigned different stimulation currents for four unit chips. We repeated steps 2) and 3) before we changed the operation mode. We successfully obtained the injection currents with the preset conditions.

Fig. 5(d) shows the demonstration result for the relaying stimulation operation. Just after the command to turn the selected unit chip (address = "00000001") into the relaying mode, the digital pulses applied on the STIM line are observed at the stimulation electrode of the unit chip "00000001."

In Fig. 5(a) and (d), we can see the output traces showing the light-controlled decision. The output signal was observed when the unit chip was illuminated. The results show that the light-controlled decision circuitry worked correctly. Fig. 6 shows the threshold light intensity as a function of the length of the last pulse for commanding. The threshold light intensity is in a reciprocal relationship with the photodiode discharge time. This result is consistent with the nature of the active pixel sensor circuitry and shows that the sensitivity (threshold light intensity) is widely adjustable. The discharge time by the dark current was typically 30 s for the present device.

IV. Image-Based Patterned Current Injection Using a Radially Aligned Retinal Stimulator

In order to verify the functionality of the image-based patterned stimulation, we performed an experimental demonstration in a "dry" situation. We used the radially aligned stimulator shown as chip (a) in Table III for the demonstration. The experiments in this section were performed with a die mounted on an 84-pin pin grid array package. We projected light patterns on the stimulator and set the function for all the unit chip cores as light-controlled stimulation with current amplitudes of 100 μA. After sending 41 sets of addressing and commanding pulses, we changed the operation mode into a stimulation mode. We then applied alternative pulses on CONT1 and CONT2 to generate the stimulation current pulses. We recorded the current profiles observed from the stimulation electrodes.

Fig. 7 shows the results of the experimentally performed image-based patterned current injection. The traces show the current profile recorded at the stimulation electrodes. The traces are placed to show the positions of the corresponding electrodes. As shown in Fig. 7, the organized unit chips work as a retinal stimulator with a functionality of image-based multisite stimulation.

V. *In Vivo* Demonstration of the Light-Controlled Stimulation on a Rabbit's Retina

We performed an *in vivo* experimental demonstration of the light-controlled retinal stimulation. We implemented the circuitry for light-controlled decisions (Fig. 3) on the previously developed multichip flexible retinal stimulator [15]–[18]. It is reasonable to use the previously developed platform and experimental protocol to demonstrate the functionality of the light-controlled stimulation.

In the present work, we used the same device packaging and experimental procedure as our previous report [18] except that we illuminated the stimulator with infrared (IR) light through the rabbit's retina. Since the rabbit (a Dutch black belted rabbit) was a wild type and its retina had not been degenerated, the wavelength chosen for the control light must be insensible by the rabbit's retina. We prepared an LED light source with a peak wavelength of 950 nm. A 3 × 3 array of IR LED (OSRAM, LD271H) was placed in front of the rabbit's eye. The distance between the implanted stimulator chip and the LED light source

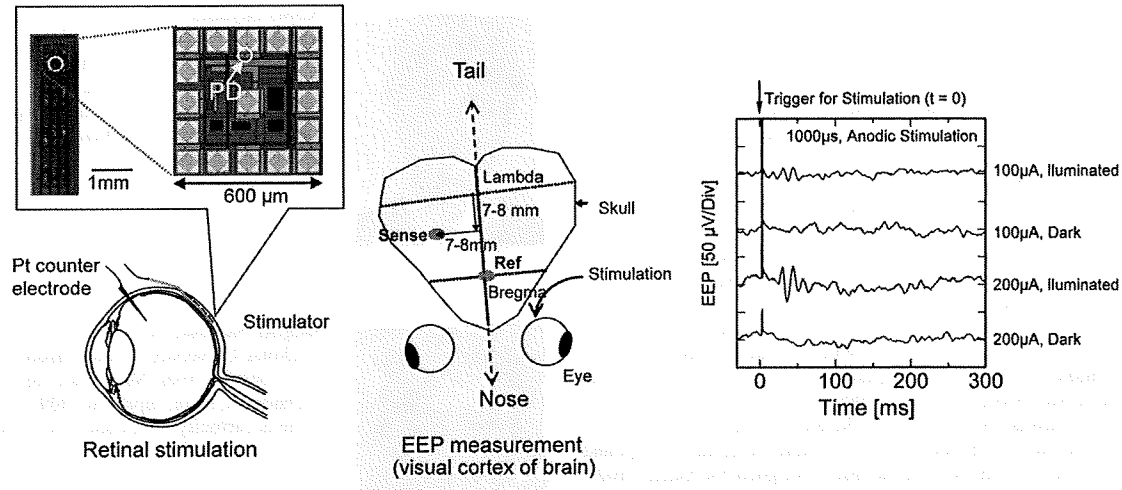

Fig. 8. Experimental setup and EEP traces observed in the *in vivo* retinal stimulation experiment using a rabbit.

was approximately 50 mm. We confirmed that no visually evoked potential (VEP) was observed by the IR illumination on the rabbit's retina.

After the surgical operation to implant the stimulator [18], we confirmed that a clear VEP response in the visual cortex of the animal's brain was observed when we used visible light. We can confirm that the rabbit was appropriately anesthetized and that the visual nerve system was ready for experiments.

In the *in vivo* experimental demonstration, we stimulated the rabbit's retina with an anodic constant-current injection. The pulse height was chosen to be between 50 and 300 μA, and the pulse duration was 1000 μs. The stimulation was performed 100 times with an interval of 2 s, and the signal on the visual cortex of the brain was averaged and recorded.

Fig. 8 shows the experimental setup [18] and results of the demonstration. The positions of the stimulator and the electrodes on the visual cortex are shown in Fig. 8. During the acute experiment, the stimulator was fixed at the insertion slit of the scleral pocket with a surgical suture. The inserted part of the stimulator was as flexible as it can fit the curvature, only with the pressure in the scleral pocket. The EEP traces show that the stimulation was successfully controlled by the IR light and caused differences in the response in the visual cortex of the rabbit's brain. For both conditions of 100 and 200 μA, clear responses were observed at 20–60 ms after the stimulation. The duration and waveform observed on the EEP traces suggest that the stimulation on the retina was enabled by only the illumination. Therefore, we can conclude that the rabbit's perception was controlled by light which was insensible to the rabbit's retina. This is a quite simple but direct demonstration of the concept for light-controlled (and image-based) retinal prosthesis. Since the spatial resolutions in both the retinal stimulation and EEP measurement on the visual cortex were limited in this paper, we cannot conclude that the sensation evoked by the current stimulator is a phosphene with a limited area. As future work, we need to perform more detailed animal experiments to confirm the functionality of evoking localized phosphenes that were observed in human experiments [14]. Biological effects in a long-term implantation are another important issue to be clarified.

VI. Conclusion

We have developed a CMOS LSI stimulator chip with the concept of a multichip architecture. The CMOS LSI stimulator system has the following features; 1) multisite stimulation using an on-chip stimulator; 2) light-controlled (imaging-based) stimulation; and 3) potential compatibility for spherical packaging. We can set different conditions for each unit chip connected to a single set of five-channel bus wiring and perform multisite constant-current biphasic retinal stimulation. We implemented a simple binary light-sensing circuitry on the unit chip to realize the image-based patterned stimulation on the retina.

We verified that all the implemented functionalities correctly work and characterize the performance of the circuitry. The demonstration for the image-based patterned current injection using radially aligned unit chips was performed in dry experiments. We also experimentally demonstrated the *in vivo* retinal stimulation based upon light-controlled decisions using light intensity measured at the stimulation site. It was a simplified demonstration for the concept of retinal prosthesis with on-site imaging.

References

[1] W. Liu and M. S. Humayun, "Retinal prosthesis," in *Proc. IEEE Int. Conf. Solid-State Circuits Dig. Tech. Papers*, Feb. 2004, pp. 218–219.

[2] L. Theogarajan, J. Wyatt, J. Rizzo, B. Drohan, M. Markova, S. Kelly, G. Swider, M. Raj, D. Shire, M. Gingerich, J. Lowenstein, and B. Yomtov, "Minimally invasive retinal prosthesis," in *Proc. IEEE Int. Conf. Solid-State Circuits Dig. Tech. Papers*, Feb. 2006, pp. 99–108.

[3] G. J. Suaning and N. H. Lovell, "CMOS neurostimulation ASIC with 100 channels, scaleable output, and bidirectional radio-frequency telemetry," *IEEE Trans. Biomed. Eng.*, vol. 48, no. 2, pp. 248–260, Feb. 2001.

[4] M. Ortmanns, N. Unger, A. Rocke, M. Gehrke, and H. J. Tietdke, "A 0.1 mm^2, digitally programmable nerve stimulation pad cell with high-voltage capability for a retinal implant," in *Proc. IEEE Int. Conf. Solid-State Circuits Dig. Tech. Papers*, Feb. 2006, pp. 89–98.

[5] A. Rothermel, V. Wieczorek, L. Liu, A. Stett, M. Gerhardt, A. Harscher, and S. Kibbel, "A 1600-pixel subretinal chip with DC-free terminals and $\pm$2 V supply optimized for long lifetime and high stimulation efficiency," in *Proc. IEEE Int. Conf. Solid-State Circuits Dig. Tech. Papers*, Feb. 2008, pp. 144–146.

[6] J. D. Loudin, D. M. Simanovskii, K. Vijayraghavan, C. K. Sramek, A. F. Butterwick, P. Huie, G. Y. McLean, and D. V. Palanker, "Optoelectronic retinal prosthesis: System design and performance," *J. Neural Eng.*, vol. 4, no. 1, pp. S72–S84, Mar. 2007.

[7] A. Butterwick, A. Vankov, P. Huie, Y. Freyvert, and D. Palanker, "Tissue damage by pulsed electrical stimulation," *IEEE Trans. Biomed. Eng.*, vol. 54, no. 12, pp. 2261–2267, Dec. 2007.
[8] T. Tanaka, K. Sato, K. Komiya, T. Kobayashi, T. Watanabe, T. Fukushima, H. Tomita, H. Kurino, M. Tamai, and M. Koyanagi, "Fully implantable retinal prosthesis chip with photodetector and stimulus current generator," in *IEDM Tech. Dig.*, 2007, pp. 1015–1018.
[9] A. Y. Chow and V. Y. Chow, "Subretinal electrical stimulation of the rabbit retina," *Neurosci. Lett.*, vol. 225, no. 1, pp. 13–16, Mar. 1997.
[10] A. Y. Chow, V. Y. Chow, K. H. Packo, J. S. Pollack, G. A. Peyman, and R. Schuchard, "The artificial silicon retina microchip for the treatment of vision loss from retinitis pigmentosa," *Arch. Ophthalmol.*, vol. 122, no. 4, pp. 460–469, Apr. 2004.
[11] E. Zrenner, D. Besch, K. U. B. Schmidt, F. Gekeler, V. P. Gabel, C. Kuttenkeuler, H. Sachs, H. Sailer, B. Wilhelm, and R. Wilke, "Subretinal chronic multi-electrode arrays implanted in blind patients," in *Proc. Shanghai Int. Conf. Physiol. Biophys.*, 2006, p. 147.
[12] F. Gekeler, P. Szurman, S. Grisanti, U. Weiler, R. Claus, T.-O. Greiner, M. Volker, K. Kohler, E. Zrenner, and K. U. Bartz-Schmidt, "Compound subretinal prostheses with extra-ocular parts designed for human trials: Successful long-term implantation in pigs," *Graefe's Arch. Clin. Exp. Ophthalmol.*, vol. 245, no. 2, pp. 230–241, Feb. 2007.
[13] K. Nakauchi, T. Fujikado, H. Kanda, T. Morimoto, J. S. Choi, Y. Ikuno, H. Sakaguchi, M. Kamei, M. Ohji, T. Yagi, S. Nishimura, H. Sawai, Y. Fukuda, and Y. Tano, "Transretinal electrical stimulation by an intrascleral multichannel electrode array in rabbit eyes," *Graefe's Arch. Clin. Exp. Ophthalmol.*, vol. 243, no. 2, pp. 169–174, Feb. 2005.
[14] M. Kamei, T. Fujikado, H. Kanda, T. Morimoto, K. Nakauchi, H. Sakaguchi, Y. Ikuno, M. Ozawa, S. Kusaka, and Y. Tano, "Suprachoroidal transretinal stimulation (STS) artificial vision system for patients with retinitis pigmentosa," *Invest. Ophthalmol. Vis. Sci.*, vol. 47, p. 1537, 2006, E-Abstract.
[15] T. Tokuda, Y.-L. Pan, A. Uehara, K. Kagawa, M. Nunoshita, and J. Ohta, "Flexible and extendible neural interface device based on cooperative multi-chip CMOS LSI architecture," *Sens. Actuators A, Phys.*, vol. 122, no. 1, pp. 88–98, Jul. 2005.
[16] J. Ohta, T. Tokuda, K. Kagawa, T. Furumiya, A. Uehara, Y. Terasawa, M. Ozawa, T. Fujikado, and Y. Tano, "Silicon LSI-based smart stimulators for retinal prosthesis," *IEEE Eng. Med. Biol. Mag.*, vol. 25, no. 5, pp. 47–59, Sep./Oct. 2006.
[17] J. Ohta, T. Tokuda, K. Kagawa, S. Sugitani, M. Taniyama, A. Uehara, Y. Terasawa, K. Nakauchi, T. Fujikado, and Y. Tano, "Laboratory investigation of microelectronics-based stimulators for large-scale suprachoroidal transretinal stimulation (STS)," *J. Neural Eng.*, vol. 4, no. 1, pp. S85–S91, Mar. 2007.
[18] T. Tokuda, R. Asano, S. Sugitani, M. Taniyama, Y. Terasawa, M. Nunoshita, K. Nakauchi, T. Fujikado, Y. Tano, and J. Ohta, "Retinal stimulation on rabbit using CMOS-based multi-chip flexible stimulator toward retinal prosthesis," *Jpn. J. Appl. Phys.*, vol. 47, no. 4, pp. 3220–3225, 2008.
[19] M. Mahadevappa, J. D. Weiland, D. Yanai, I. Fine, R. Greenberg, and M. S. Humayun, "Perceptual thresholds and electrode impedance in three retinal prosthesis subjects," *IEEE Trans. Neural Syst. Rehabil. Eng.*, vol. 13, no. 2, pp. 201–206, Jun. 2005.
[20] J. W. Morley, Y. T. Wong, L. E. Hallum, S. C. Chen, N. Dommel, S. L. Cloherty, G. J. Suaning, and N. H. Lovell, "Optical imaging of electrically evoked visual signals in cats: I. Responses to corneal and intravitreal electrical stimulation," in *Proc. 29th Annu. Int. Conf. IEEE Eng. Med. Biol. Soc.*, Aug. 2007, pp. 1635–1638.

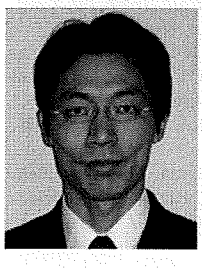

Takashi Tokuda (M'08) received the B.E. and M.E. degrees in electronic engineering and the Dr.Eng. degree in materials engineering from Kyoto University, Kyoto, Japan, in 1993, 1995, and 1998, respectively.

He has been an Assistant Professor since 1999 and has been an Associate Professor since 2008 with the Graduate School of Materials Science, Nara Institute of Science and Technology, Nara, Japan. His research interests include CMOS image sensors, bioimaging, and biosensors.

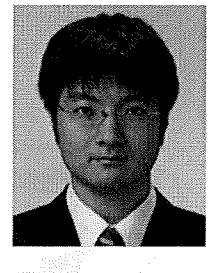

Kohei Hiyama received the B.E. degree from Osaka Kyoiku University, Osaka, Japan, in 2007 and the M.E. degree from Nara Institute of Science and Technology, Nara, Japan, in 2009.

He is currently with the Corporate Manufacturing Engineering Center, Toshiba Corporation, Yokohama, Japan.

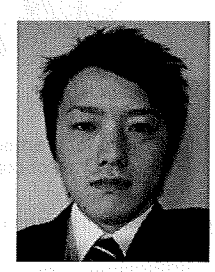

Shigeki Sawamura received the B.E. degree from Ryukoku University, Kyoto, Japan, in 2007 and the M.E. degree from Nara Institute of Science and Technology, Nara, Japan, in 2009.

He is currently with Canon Inc., Tokyo, Japan.

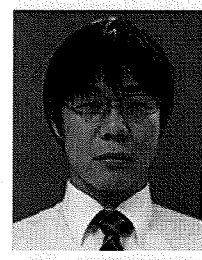

Kiyotaka Sasagawa (M'08) received the B.S. degree from Kyoto University, Kyoto, Japan, in 1999 and the M.E. and Ph.D. degrees in materials science from Nara Institute of Science and Technology, Nara, Japan, in 2001 and 2004, respectively.

From 2004 to 2008, he was a Researcher with the National Institute of Information and Communications Technology, Tokyo, Japan. In 2008, he joined Nara Institute of Science and Technology, where he is currently an Assistant Professor. His research interests involve bioimaging, biosensing, and electromagnetic field measurement.

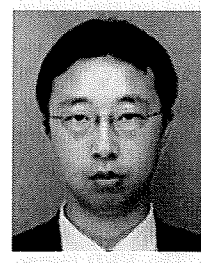

Yasuo Terasawa received the B.E. and M.E. degrees from Tohoku University, Sendai, Japan, in 1996 and 1998, respectively, and the Ph.D. degree from Nara Institute of Science and Technology, Nara, Japan, in 2009.

He is currently with the Vision Institute, R&D Division, NIDEK Company, Ltd., Gamagori, Japan.

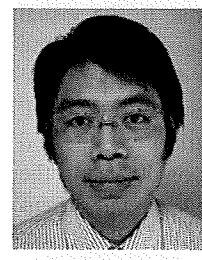

Kentaro Nishida received the M.D. degree from Osaka University, Osaka, Japan, where he is currently working toward the Ph.D. degree.

Yoshiyuki Kitaguchi received the M.D. degree from Osaka University, Osaka, Japan, where he is currently working toward the Ph.D. degree.

His research interests include evaluating retinal damages with a retinal imaging device, i.e., adaptive optics fundus camera.

Takashi Fujikado received the B.E. and M.E. degrees from The University of Tokyo, Tokyo, Japan, and the M.D. and Ph.D. degrees from Osaka University, Osaka, Japan.

He is currently a Professor of applied visual science with the Graduate School of Medicine, Osaka University. He has been involved in the field of neuro-ophthalmology and ophthalmic optics.

Dr. Fujikado is a member of the Consortium of Artificial Retina in Japan, where he is working on the functional assessment of artificial retina.

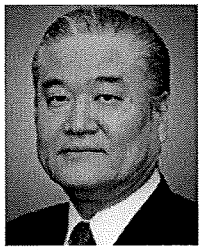

Yasuo Tano received the M.D. and Ph.D. degrees from Osaka University, Osaka, Japan.

He was with the Department of Ophthalmology, Graduate School of Medicine, Osaka University. He conducted the Retinal Prosthesis Project Team consisting of Osaka University, Nara Institute of Science and Technology, Nara, Japan, and Nidek Company, Ltd.

Dr. Tano was the former President of the Japanese Ophthalmological Society and was the current President of Asia Pacific Academy of Ophthalmology. He passed away on January 31, 2009.

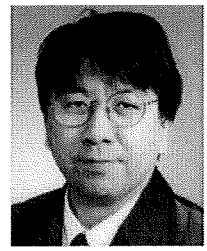

Jun Ohta (M'97) received the B.E., M.E., and Dr.Eng. degrees in applied physics from The University of Tokyo, Tokyo, Japan, in 1981, 1983, and 1992, respectively.

In 1983, he joined Mitsubishi Electric Corporation, Hyogo, Japan, where he has been engaged in the research on optoelectronic integrated circuits, optical neural networks, and artificial retina chips. From 1992 to 1993, he was a Visiting Researcher with the Optoelectronics Computing Systems Center, University of Colorado, Boulder. Since 1998, he has been an Associate Professor with the Graduate School of Materials Science, Nara Institute of Science and Technology, Nara, Japan, where, since 2004, he has been a Professor. His current research interests include vision chips, complimentary metal–oxide–semiconductor image sensors, retinal prosthesis devices, biophotonic large-scale integrations, and integrated photonic devices.

Sensors **2009**, *9*, 9073-9093; doi:10.3390/s91109073

OPEN ACCESS

sensors

ISSN 1424-8220

www.mdpi.com/journal/sensors

Review

Implantable CMOS Biomedical Devices

Jun Ohta [1,2,*], Takashi Tokuda [1,2], Kiyotaka Sasagawa [1,2] and Toshihiko Noda [1,2]

[1] Nara Institute of Science and Technology, 8916-5 Takayama, Ikoma, Nara 630-0101, Japan

[2] CREST, Japan Science and Technology Agency, 3-5 Sanban, Chiyoda, Tokyo 102-0075, Japan; E-Mails: tokuda@ms.naist.jp (T.T.); sasagawa@ms.naist.jp (K.S.); t-noda@ms.naist.jp (T.N.)

* Author to whom correspondence should be addressed; E-Mail: ohta@ms.naist.jp; Tel.: +81-743-72-6051; Fax: +81-743-72-6059.

Received: 5 August 2009; in revised form: 6 November 2009 / Accepted: 9 November 2009/ Published: 17 November 2009

Abstract: The results of recent research on our implantable CMOS biomedical devices are reviewed. Topics include retinal prosthesis devices and deep-brain implantation devices for small animals. Fundamental device structures and characteristics as well as *in vivo* experiments are presented.

Keywords: biomedical devices; retinal prosthesis; image sensors; CMOS; brain implantation

1. Introduction

The trend toward ultra-fine scale in CMOS technologies has not only increased chip integration density but has also enabled the widespread application of CMOS technologies in areas such as image sensors, wireless, micro-electro-mechanical systems (MEMS), and micro total analysis system (μTAS). These features are suitable for biomedical applications. For example, implantable devices require small volume and low power consumption, which are realized by ultra-fine fabrication technology. MEMS are effective technologies for biomedical applications, because MEMS easily form three-dimensional structured which are useful in the applications. Image sensor technology is also very efficient for biotechnology applications in which fluorescence is frequently used for labeling specific cells or detecting neural activity. CMOS technologies are thus highly suitable for implantable devices for biomedical applications and have been used in various types of devices.

In this review, two typical examples of implantable CMOS devices from our research are described: retinal prosthesis devices [1-5] and brain-implantable devices based on CMOS technologies [6-9]. In retinal prosthesis devices, MEMS technologies with CMOS circuits have been used to realize a retinal stimulator based on a microchip array, and in brain-implantable devices, image sensor technology and MEMS have been combined to realize an ultra-compact device to be implanted in the deep brain of experimental small animals. The present review describes the results of recent research on retinal prosthesis devices and brain-implantable devices. In Chapter 2, we discuss the advantages and problems associated with the *in vivo* implantation of CMOS devices. In Chapter 3, we describe retinal prosthesis devices that we have developed. We also describe a multiple microchip architecture that we developed in order to realize a retinal stimulator that uses a large number of stimulus electrodes while bending the stimulator to match the curvature of an eyeball. Chapter 4 describes brain-implantable CMOS imaging devices for measuring the neural activity in the deep brain of a small experimental animal, such as a mouse. Chapter 5 briefly addresses areas for future research and summarizes the present review.

2. *In Vivo* Implantation of CMOS Devices

This section describes the advantages and problems associated with *in vivo* implantation of CMOS devices. Figure 1 summarizes these advantages and problems. The advantages include high performance and versatile functionality in the detection of bio-signals and the stimulation of living cells by on-chip integration of circuits. For example, an on-chip amplifier can detect weak signals with a high signal-to-noise (SN) ratio, and an on-chip multiplexer can be used for multi-site stimulation.

Figure 1. Advantages and problems associated with *in vivo* implantation of CMOS devices.

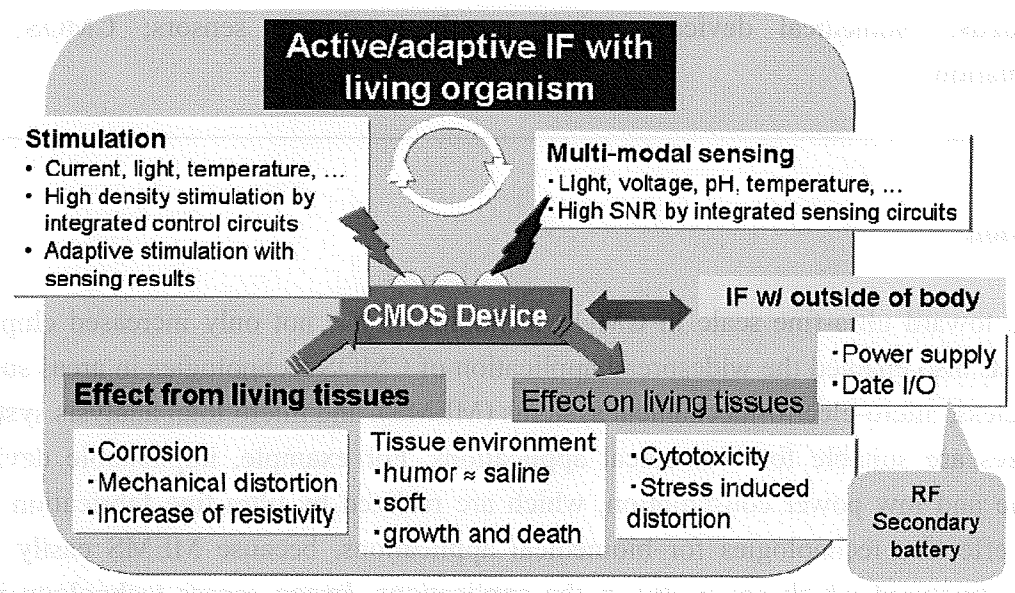

CMOS devices also have the advantage of multi-modal sensing of, for example, physical values such as the amount of light, voltage, and temperature, ions, and chemical entities such as enzymes. CMOS devices also enable multi-modal stimulation such as injection of charge and chemical

substances. The important point is that a CMOS device can configure a closed-loop of sense and stimulation. Neural cells can be actively and adaptively stimulated by detecting physical value(s) and analyzing spatio-temporal dynamics. For example, in retinal prosthesis, retinal cell stimulation is often adaptively controlled by monitoring the impedance value. In addition, for deep brain stimulation, such an implanted device is proposed that monitors the amount of dopamine emitted in a patient's brain, determines the optimum value of stimulation, and stimulates the deep brain before the onset of tremor is currently being developed [10]. This is a typical example of a closed-loop device.

Although implanted CMOS devices are expected to provide a highly sophisticated interface with the living body, there are many problems to be solved before realization because both stable and safe operation *in vivo* is required. Figure 1 shows these issues. An implanted device affects living tissues or cells, and these effects can include cytotoxicity and stress-induced distortion. As for cytotoxicity, packaging materials and/or electrode materials may be dissolved into tissue and affect cells. Many discussions including cytotoxicity and mechanical distortions appear in [11]. In addition, in stimulation, electrochemical reactions can occur when the stimulation voltage exceeds the voltage window, and pH changes and/or bubbling can have harmful effects on neural cells [12,13]. Moreover, implanted devices are also affected by the living environment. The living environment is composed primarily of saline solution, so that a CMOS chip with no coating may be damaged. Therefore, a highly water-tight packaging is necessary such as parylene. Of course, this material must be biocompatible. An implanted device is stressed by the living tissues so that it may be distorted or broken. For example, a thinned CMOS chip is easily implanted but may be broken by stress from tissues because Si is fragile when thinned. Living tissues may grow and die, and thus the configuration between the device and tissues may change gradually. This may cause an impedance change between an electrode and living cells. Implanted devices must be designed knowing that the configuration of the device may change.

Figure 2. Electrical stimulation of neural cells in body fluid (a) and its equivalent circuits (b).

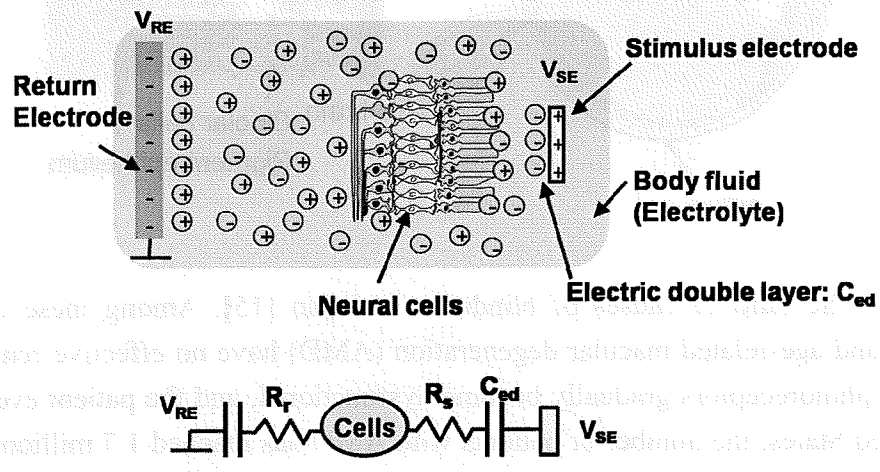

Next, we consider the stimulation of neural cells in, for example, artificial cochlear and retinal prostheses. In these applications, stimulation is achieved by extra cellular stimulation, in which the potential between the inside and outside of the cell is changed through electrolytes such as a body fluid.

Consequently, when a voltage is applied to a stimulus electrode, an electric double layer is produced near the electrode. The thickness of this layer is very thin so that the associated capacitance is large. Resistance also exists in the electrolyte. The equivalent circuits are shown in Figure 2. The impedance between the electrode and the cells may change if the distance between the electrode and the cells changes, as mentioned previously. Stimulation is achieved with a short voltage pulse. This voltage pulse is made biphasic, that is, two consecutive pulses of opposite polarity to achieve charge balance and to deliver a zero net charge into the tissue to ensure long-term safety. In addition, for the purpose of achieving charge balance, a biphasic pulse is usually used to ensure long-term safety. A biphasic pulse consists of two opposite polarity pulses, which deliver no net charges into tissues.

3. Retinal Prostheses

3.1. Blindness

As shown in Figure 3, the human retina is a thin, layered tissue with a thickness of 0.1–0.4 mm attached to the inner surface of the eyeball [14]. The retina has a layered structure with photoreceptor cells for light detection in the bottom layer and ganglion cells for output in the top layer. The retina plays an important role in visual information collection and processing, and so dysfunction can result in blindness.

Figure 3. Schematic illustration of the structure of the eye and retina.

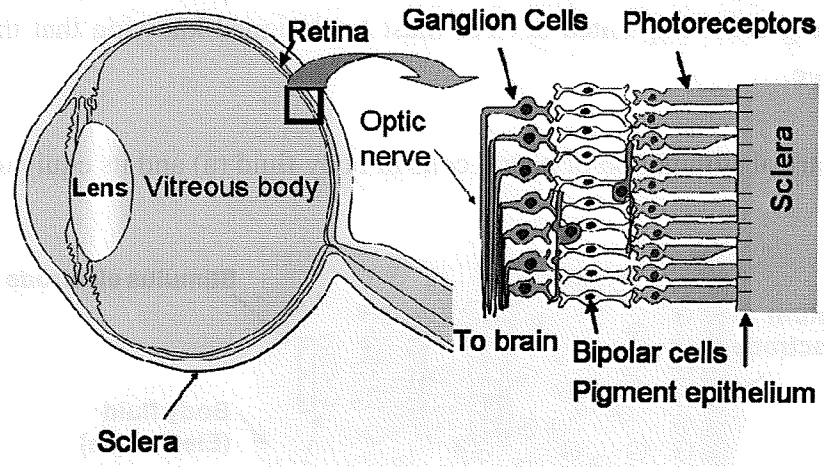

Figure 4 shows the ratio of causes of blindness in Japan [15]. Among these diseases, retinitis pigmentosa (RP) and age-related macular degeneration (AMD) have no effective remedies at present. In both cases, the photoreceptors gradually become dysfunctional, and the patient eventually becomes blind. In the United States, the number of patients with AMD has reached 1.7 million, which accounts for the majority of cases of disease-related blindness, and this number increases by some 155,000 every year. Within 25 years, the number of patients with AMD will reach 5.1 million. As such, a cure for AMD must be found as soon as possible.

Figure 4. Ratio of causes of blindness in Japan (adapted from [15]).
AMD: age-related macular degeneration. RP: retinitis pigmentosa.

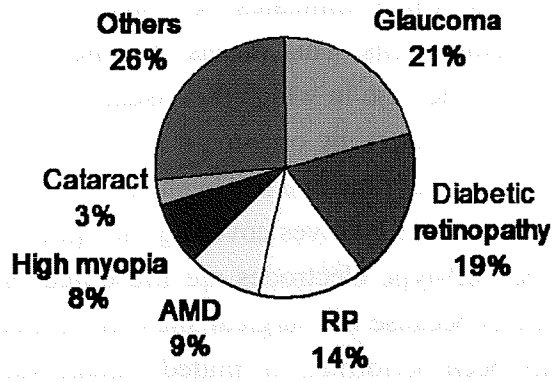

3.2. Principle of Retinal Prosthesis and Types of Stimulation Sites

In RP and AMD, photoreceptor cells are dysfunctional, but most of the other retinal cells, such as ganglion cells, are still alive, unless the disease is in the terminal stage [16,17]. Consequently, by stimulating the remaining retinal cells, visual sensation or phosphene can be evoked. This is the principle of the retinal prosthesis or artificial vision. Based on this principle, a retinal prosthesis device stimulates retinal cells with a patterned electrical signal so that a blind patient may sense a patterned phosphene, or something like an image.

Figure 5. Stimulation sites of the retinal prosthesis.

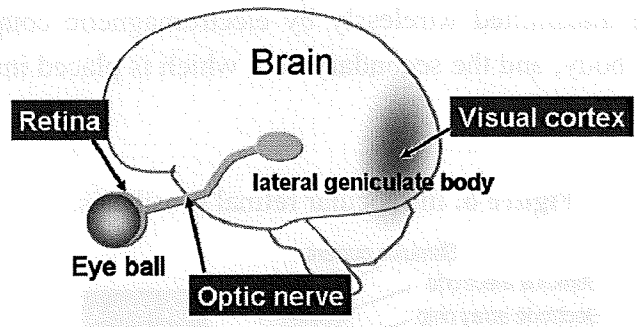

According to the site at which the retinal stimulator is placed, the retinal prosthesis device is classified into three categories: epi-retinal stimulation [18-21], sub-retinal stimulation [22-25], and suprachoroidal transretinal stimulation (STS) [25,26], which has recently been developed. The stimulation site may be located not only in retinal cells, but also in the pathways to the brain, such as the optic nerves [27], which are the transmission lines of visual information, and, of course, in the visual cortex [28], which is the terminal of the visual information. Figure 5 shows the arrangement of these elements.

In the present review, a prosthesis for which the stimulator is located inside or near the eyeball is referred to as an intraocular retinal prosthesis, and prostheses that involve optic nerve stimulation or visual cortex stimulation, for example, are referred to as extraocular retinal prostheses. These prostheses have certain advantages and disadvantages, which are described below.